Adhesion strength of piles in saline ice

Inoue, M.; Frederking, R. M. W.

National Research Council Canada
Conseil national de recherches Canada

Institute for Research in Construction
Institut de recherche en construction

(11)

Adhesion Strength of Piles in Saline Ice

by M. Inoue and R. Frederking

Appeared in
Proceedings 8th International IAHR Symposium on Ice
Iowa City, Iowa, August 18-22, 1986
Vol. III, p. 89-104
(IRC Paper No. 1502)

Price $3.00

NRCC 28603

Canada

RÉSUMÉ

On a effectué des essais en laboratoire pour étudier les effets de la vitesse de déplacement, de l'épaisseur de glace et du diamètre des pieux sur l'adhérence d'une couche de glace saline sur des pieux de bois. La glace utilisée était représentative de la glace de mer à grains prismatiques formée naturellement. Des pieux cylindriques de diamètre variant entre 30 et 145 mm ont été extraits à des vitesses de déplacement nominales constantes se situant entre $1,5 \times 10^{-4}$ et $7,8 \times 10^{-2}$ mm/s, l'épaisseur de la glace allant de 58 à 170 mm.

On a constaté que le mode de rupture, soit par cisaillement à l'interface pieu-glace, soit par flexion de la glace, dépendait des paramètres des essais. La force d'adhérence augmentait de façon proportionnelle au déplacement des pieux et à l'épaisseur de la glace, et de façon inversement proportionnelle au diamètre des pieux. On a observé que l'adhérence de la glace saline était au moins 3,5 fois moins grande que celle, mesurée antérieurement dans des conditions semblables, de la glace d'eau douce à grains prismatiques.

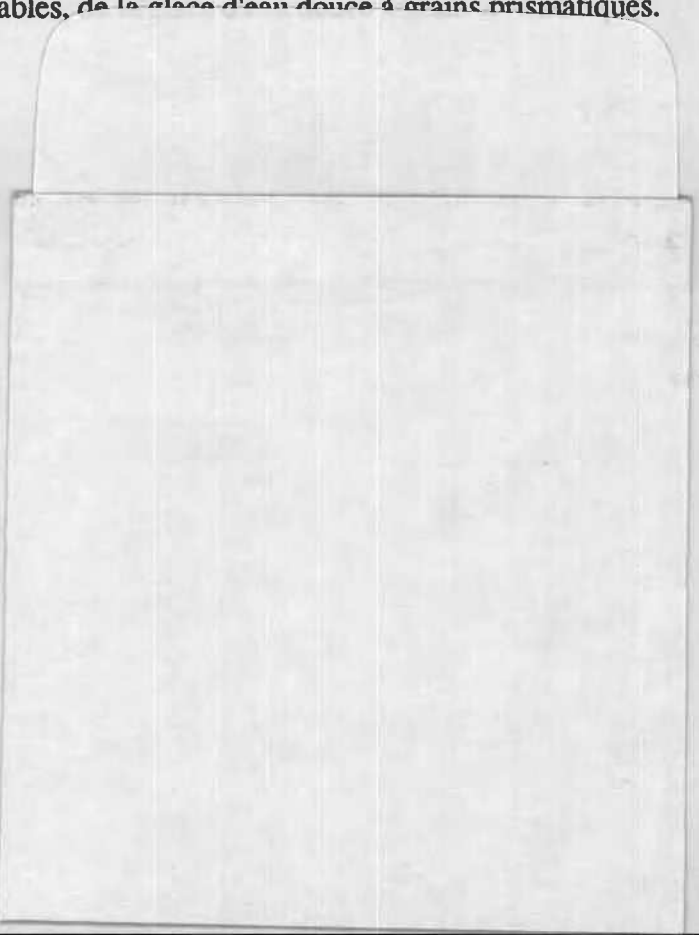

IAHR Ice Symposium 1986
Iowa City, Iowa

ADHESION STRENGTH OF PILES IN SALINE ICE

M. Inoue — Ice Engineering Lab.,Tsu Research Center, Nippon Kokan K.K. — Japan

R. Frederking — Institute for Research in Construction, National Research Council — Canada

ABSTRACT

Laboratory tests were conducted to investigate the effects of displacement rate, ice thickness and pile diameter on the adhesion of a saline ice sheet to wooden piles. The ice used was representative of naturally formed columnar-grained sea ice. Cylindrical piles having diameters between 30 and 145 mm were pulled up at constant nominal displacement rates between $1.5X10^{-4}$ and $7.8X10^{-2}$ mm/sec, for ice thicknesses from 58 to 170 mm.

The failure mode, either shear at the pile-ice interface or flexural in the ice was observed to depend upon the test parameters. The adhesion strength was observed to increase with increasing pile dispalcement rate, increasing ice thickness and decreasing pile diameter. The adhesion strength of saline ice was found to be smaller by a factor of at least 3.5 than that of freshwater columnar-grained ice measured earlier under similar conditions.

1. INTRODUCTION

A floating ice cover develops substantial vertical loads on a structure to which it is frozen due to changes in water level. This type of load is an impotant factor in design and construction of arctic offshore structures used in petroleum exploration and production. It is, therefore, necessary to evaluate such vertical ice loads acting on a structure surrounded by sea ice, in relation to adfreeze bond between material and ice.

Sackinger and Sackinger (1977) subjected a steel cylinder embeded in sea ice to an applied torque and measured the adhesion strength as a function of salinity and temperature. Saeki et al. (1981) conducted push-out tests on piles with various materials in sea ice, and measured the adhesion strength as a function of pile displacement rate, diameter and material as well as ice thickness and temperature. Oksanen (1982) measured adhesive shear strength between saline ice and steel plates under varying salinities and relatively low temperatures. These investigations were related to the case where shear between the material and ice predominates. Under natural conditions, however, the ice cover could fail in bending as well as shear. On the other hand, theoretical treatments of vertical ice loads on piles have been based on the bending theory of a plate on an elastic foundation (for example, Lofquist, 1951). Recently Vershinin et al. (1983) conducted field tests to determine vertical loads on 1 m diameter pile frozen into natural sea ice of 1.15m thickness. They found that the measured value of 70 tons was several times greater than the value computed according to the recommendations in the Construction Norms and Regulations (1975).

The purpose of the present work was to obtain data on the adhesion strength of piles in saline ice under conditions similar to those in nature. The tests were conducted using a relatively small tank. Piles frozen into saline ice were pulled upwards relative to the ice cover. Wooden piles were used to minimize the ice thickening effect around piles. This paper reports the test results of adhesion strength measured as a function of pile displacement rate, ice thickness and pile diameter. An empirical equation to predict the adhesion strength is also proposed.

2. DESCRIPTION OF TEST APPARATUS

Tests were conducted using a small insulated tank, 660 mm in diameter and 600 mm deep, placed in a cold room. The tank had heating tapes on the

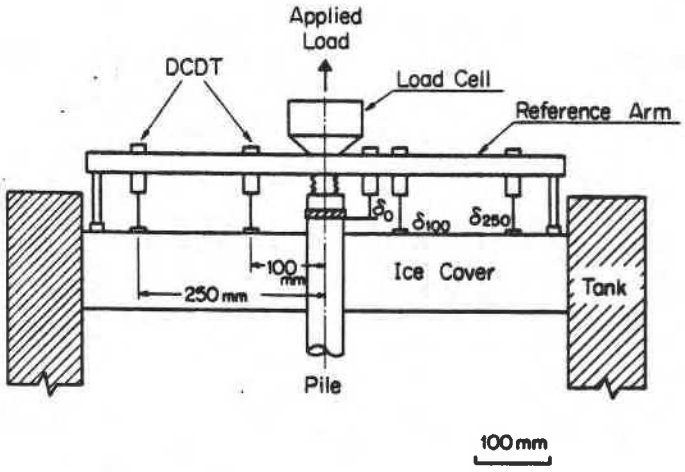

Fig.1
Scheme of load and deflection measurements

bottom and sides so that the water temperature and ice growth rate could be controlled. A thermocouple probe was used to monitor ice and water temperatures.

A loading apparatus set up over the tank pulled the pile upwards relative to the ice cover. The outer perimeter of the ice cover adhered to the tank wall liner made of galvanized steel. Load was applied with a screw jack driven by a variable speed motor. Loading speed could be varied between $7X10^{-5}$ mm/sec and $8X10^{-2}$ mm/sec. A schematic of the arrangement for measuring load and deflection of the ice cover is shown in Fig.1. Loads were measured by a load cell mounted between the pile and the screw jack. Displacement of the pile and deflections of the ice cover at radii of 100 mm and 250 mm from the center of the pile, were measured relative to the ice surface at a distance of about 25 mm from the wall of the tank, using five displacement transducers (direct current differential transformers), mounted on a reference arm. Load and displacement signals were recorded on a strip chart recorder as well as in a digitalized form.

The piles were made of B. C. fir, the same as those used earlier by Frederking (1979) for tests in freshwater ice. They were shaped on a lathe and finished by emery paper. A rod threaded through the center of the pile connected it to the load cell.

3. TEST PROCEDURE

The loading system was set over the water-filled tank. The pile was soaked and then attached to the system, carefully aligning it vertically, before ice growth was initiated. All tests were done in saline ice grown to simulate natural sea ice. The tank which was filled with water of about 22‰ salinity was located in a cold room with an ambient temperature

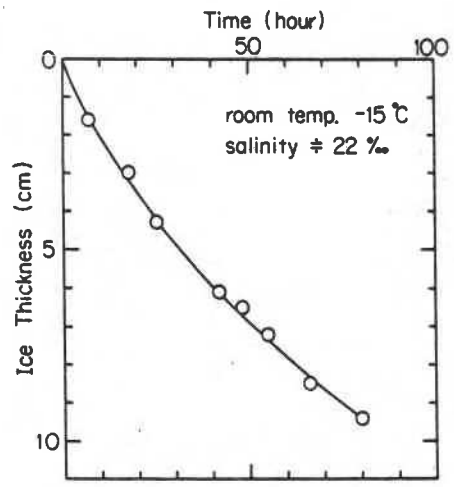

Fig.2 Ice growth as a function of time

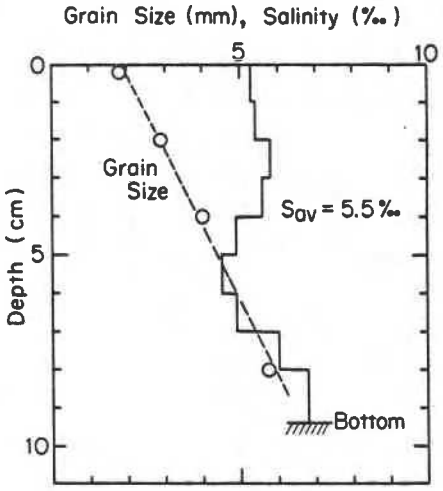

Fig.3 Grain size and salinity profiles of ice cover

of -15 ℃. The water was mixed while cooling until the entire depth reached its freezing point. When the water temperature near the surface decreased slightly below the freezing point, the tank was seeded by sieving fine-grained snow uniformly over the water surface. Side and bottom heaters helped to maintain uniform ice thickness and to prevent any ice particles from forming at the bottom of the tank during ice growth.

Fig.2 shows ice thicknesses measured with a resistance wire thickness gauge as a function of time. The growth rate varied from 40 to 20 mm/day with elapsed time. The salinity profile of the ice cover grown in this manner is shown in Fig.3, together with grain size profile. The average salinity of the ice was 5.5‰ which is quite similar to that of natural sea ice, as observed by Nakawo and Sinha (1981). The grain size increased linearly with depth, which is also similar to natural conditions observed by Weeks and Hamilton (1962). The ice consisted of a 7 mm seeded layer at the top with a columnar-grained structure extending below it. Therefore, the ice grown in the laboratory was very similar to naturally formed sea ice.

When the ice cover reached the desired thickness, the reference arm was placed onto the ice surface and displacement transducers were carefully set up. After stabilizing the transducers for about one hour, tests were started. Most of the tests were conducted at a thickness of about 90 mm and at a pile diameter of 50 mm. Nominal pile displacement rates were varied from 1.5×10^{-4} to 7.8×10^{-2} mm/sec.

4. TEST RESULTS AND DISCUSSION

A total of 21 tests were performed to investigate the effects of pile displacement rate, pile diameter and ice thickness on adhesion strength. Continous records of load and deflections with time were made for all tests. Immediately before and after each test temperature profiles of the ice cover were also measured. An example of the profile is shown in Fig.4. Average ice temperature was maintained at about -4 °C, with very little variation during a test. Test results and conditions are summarized in Table 1.

Several different types of loading curve were observed. The stress- and displacement-time curves for one type of loading behaviour are shown in Fig.5. Adhesion stress was determined by dividing the vertical load by the contact area

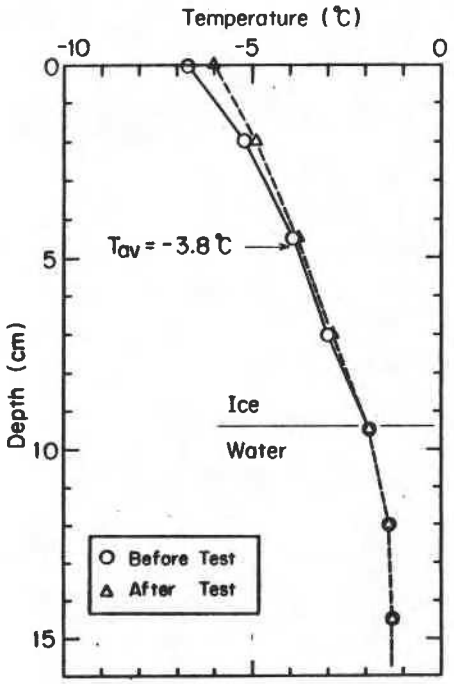

Fig.4 Temperature profile in test No.2

Table 1. TEST RESULTS

Test No.*	d (mm)	h (mm)	$\dot{\delta}_n$ (mm/sec)	τ (kPa)	t_f (sec)	δ_{fo} (mm)	δ_{f100} (mm)	δ_{f250} (mm)	r (kPa)	T_{av} (°C)	S_{av} (‰)
1R	50	95	$1.3X10^{-2}$	206	288	1.556	0.699	0.097	50	-4.4	6.4
2R	50	94	$3.5X10^{-2}$	130	408	2.175	0.933	0.095	35	-3.8	5.5
3R	50	133	$1.3X10^{-2}$	167	178	0.683	0.248	0.032	42	-4.8	4.6
4R	50	98	$7.8X10^{-2}$	134	282	1.365	0.635	0.046	—	-3.9	5.7
5NC	50	92	$2.0X10^{-3}$	63	320	0.283	0.140	0.022	—	-4.2	5.4
6RC	50	58	$1.3X10^{-2}$	80	1100	> 5	> 5	0.44	—	-3.2	5.7
7R	50	80	$8.0X10^{-3}$	146	320	1.431	0.746	0.063	—	-4.5	5.7
8RC	50	64	$1.3X10^{-2}$	113	1696	18.564	12.814	0.80	—	-3.7	6.4
9NC	50	170	$1.3X10^{-2}$	220	152	0.537	0.142	0.024	66	-5.3	5.1
10R	50	101	$8.0X10^{-3}$	150	216	0.697	0.320	0.049	53	-4.4	5.3
11R	50	85	$5.9X10^{-3}$	128	546	1.974	0.939	0.080	38	-4.4	—
12R	50	90	$3.5X10^{-3}$	124	1280	3.196	1.713	0.104	31	-4.1	6.0
13R	50	78	$1.5X10^{-3}$	84	1718	1.904	0.842	0.039	36	-4.3	6.4
14R	50	130	$1.5X10^{-3}$	89	565	0.459	0.136	——	40	-4.3	6.0
15R	50	95	$2.0X10^{-2}$	176	226	2.828	1.574	0.113	42	-4.0	6.8
16NC	50	108	$7.0X10^{-4}$	67	2521	0.764	0.167	0.056	—	-4.2	5.9
17NC	50	96	$3.5X10^{-4}$	33	6027	1.419	0.232	0.045	29	-3.8	5.5
18NC	50	95	$1.5X10^{-4}$	23	27270	2.692	0.291	0.127	—	-4.0	5.4
19R	100	98	$1.3X10^{-2}$	141	356	2.432	1.523	0.126	31	-4.2	4.6
20R	145	99	$1.3X10^{-2}$	109	278	2.118	1.186	0.146	15	-4.2	6.1
21NC	30	100	$1.3X10^{-2}$	253	109	0.691	0.267	0.033	62	-3.9	5.4

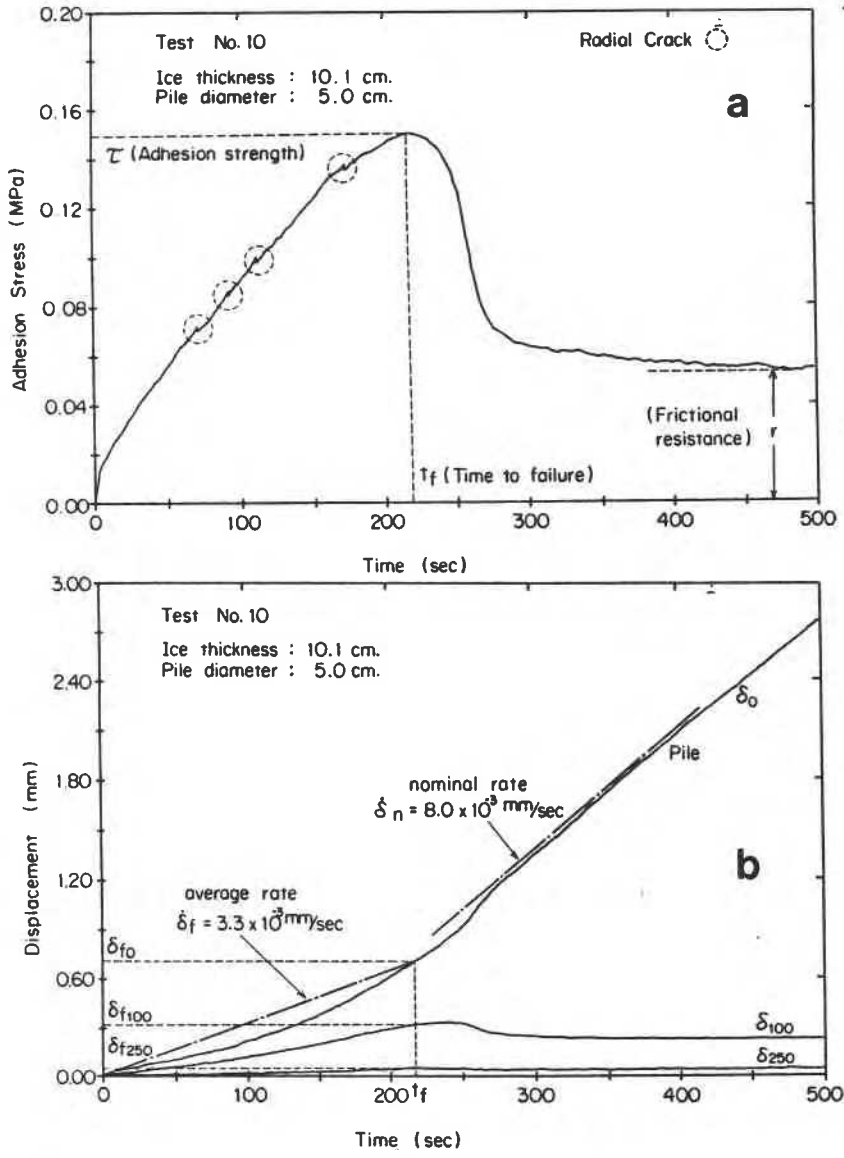

Fig.5
Records of test No.10

(a) stress-time curve

(b) displacement -time curve

between pile and ice cover. Note that the actual pile displcement rate increases with time until the stress reaches a peak, and then remains constant in the post yield region (Fig.5 (b)). The constant rate is equal to the nominal rate, which corresponds to the rate of the loading apparatus operated under no load resistance. A similar variation in rate was observed by Sinha (1981) for ice under uniaxial compression at constant nominal cross-head rates on a conventional test machine. The deflections measured at radii of 100 mm and 250 mm from the pile center also indicated the same trend until the stress reached a peak. In the present tests, the displacement and deflections were measured with a reference arm whose end points rested on the ice surface 25 mm from the inner wall of the tank. The deflection at the end point was also measured by a dial gauge attached to the tank wall, which showed that the end point was quite stationary and that if any, its deflection was at least an order

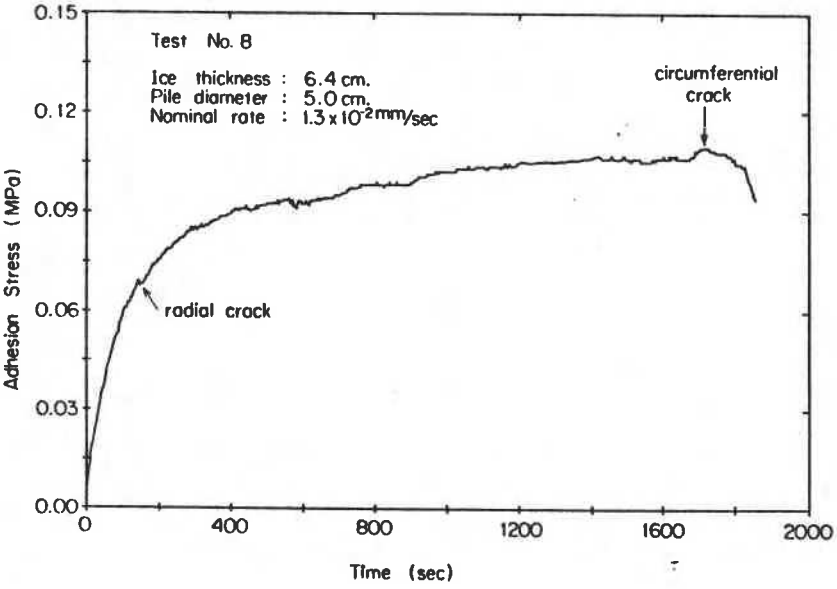

Fig.6
Stress-time curve
of test No.8

of magnitude smaller than at 250 mm radius.

Fig.5 (a) shows that as the pile is displaced upward, the stress increases monotonically reaching a maximum, and then gradually decreases to an almost constant value. Four radial cracks, circled saw-tooth-like peaks, are noted on the stress-time curve. Although no cracks were seen for the first three peaks, the sounds were heard clearly. The fourth peak corresponded to a radial crack which was visible in the ice immediately adjacent to the pile. At the maximum stress, a few additional radial cracks appeared which developed to depths limited to about 5 mm from the ice surface. Frederking (1979) has reported the development of micro cracks and a conical failure surface at a maximum load for freshwater ice tests. Such a conical failure surface was not apparent in the present tests. After the maximum stress, the adhesion between the pile and the ice was greatly diminished and friction between them became predominant. This frictional resistance was observed to be less than the peak value by a factor of 2 to 4. In the case of test No.10 the maximum stress was associated with the occurrence of radial cracks. This is designated as R in Table 1. In some cases, radial cracks could not be seen even at a maximum stress, although they could be heard. This case is designated as NC, but the failure process could be similar to the case designated R. It was difficult to see the visible cracks in the cloudy saline ice.

Fig.6 represents the stress-time curve for test No.8, which is characterized by radial cracks and subsequent circumferential crack. The peak stress corresponded to the formation of a circumferential crack. This is designated as RC in Table 1.

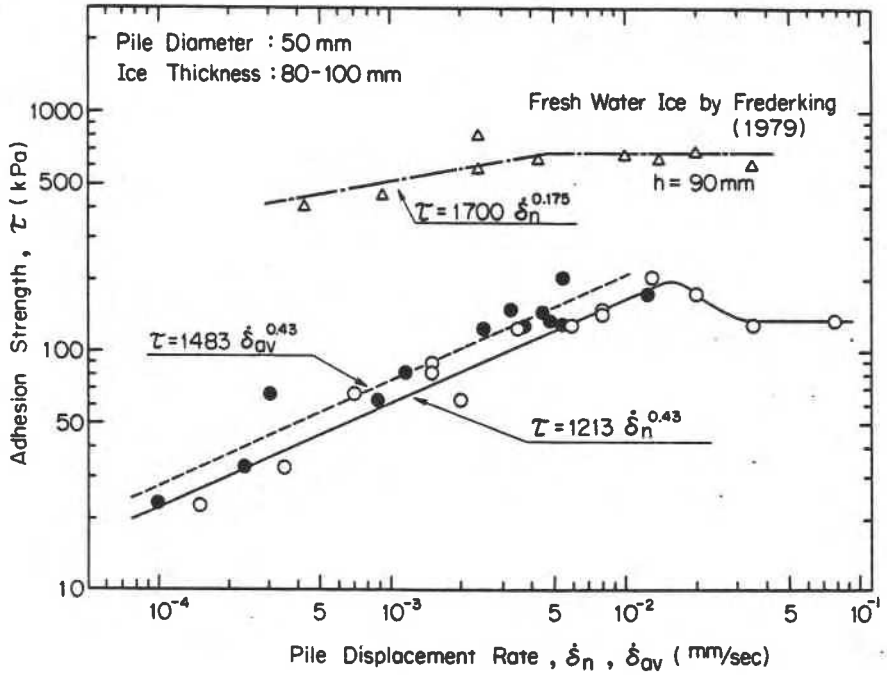

Fig.7 Adhesion strength as a function of pile displacement rate

Pile displacement rate effects

In Fig. 7 the values of adhesion strength, τ, determined from the maximum stress from curves such as Fig.5 (a) are plotted against the nominal pile displacement rates, $\dot{\delta}_n$, for a pile diameter of 50 mm and ice thickness of around 90 mm, at an average ice temperature of -4 °C. The strength increases with increase in nominal rate up to $1.5X10^{-2}$ mm/sec, then decreases sightly and remains constant. The trend is almost the same as that observed for freshwater ice by Frederking (1979), shown in the figure for comparison purposes. The adhesion strength in saline ice is smaller than that in freshwater ice, by a factor of 3.5 at higher rates corresponding to the maximum strengths. The difference becomes greater as the nominal rate decreases.

Regression analysis of the data for nominal rates less than $1.5X10^{-2}$ mm/sec gave the following equation:

$$\tau = 1213 \ \dot{\delta}_n^{0.43} \qquad (1)$$

where τ is in kPa and $\dot{\delta}_n$ is in mm/sec.

As seen in Fig.5 (b), a constant displacement rate is not achieved before yielding, so that it is more appropriate to use an average displacement rate, $\dot{\delta}_{av}$, determined by dividing the pile displacement at failure, δ_{fo}, by the time to failure, t_f. These data are plotted as filled circles in Fig.7. A regression line fitted to the data of average

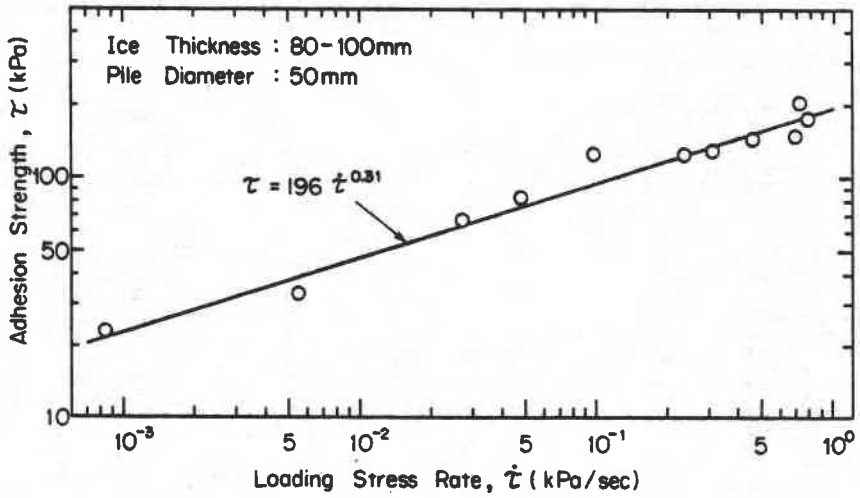

Fig.8 Adhesion strength as a function of average stress rate

rates lies to the left as compared to the previously determined regression line, on a nominal-rate basis. It is interesting to note that the data points of nominal rates higher than $2X10^{-2}$ mm/sec shift to the left significantly. This could be due to the limitation of the loading system employed in the present test series.

The rate senstivity of strength of ice, is often expressed in terms of stress rate for engineering purposes. Fig.8 shows the variation of the average stress rate, $\dot{\tau}$, (defined as adhesion strength, τ, divided by the time to failure, t_f) for the same conditions as shown in Fig.7. The adhesion strength increases linearly with increasing average stress rate, on a log-log scale. The following regression line was obtained,

$$\tau = 196\ \dot{\tau}^{0.31} \qquad (2)$$

where τ is in kPa and $\dot{\tau}$ is in kPa/sec.

Ice thickness effects

The dependence of adhesion strength on ice thickness was studied using the 50 mm diameter pile data at nominal pile displacement rates of $1.3X10^{-2}$ mm/sec and $1.5X10^{-3}$ mm/sec. The results are given in Fig.9. Most of these tests were conducted at $1.3X10^{-2}$ mm/sec since a maximum adhesion strength appeared at this rate. Although the data are small in number and scatter greatly, a regression analysis gives the following best fit equation to the data

$$\tau = 3.8\ h^{0.8} \qquad (3)$$

where τ is in kPa and h is in mm.

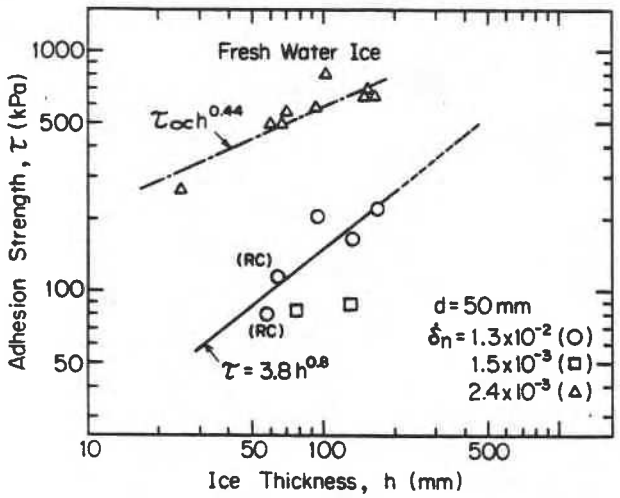

Fig.9 Adhesion strength versus Ice thickness.
RC indicates failure followed by circumferential crack

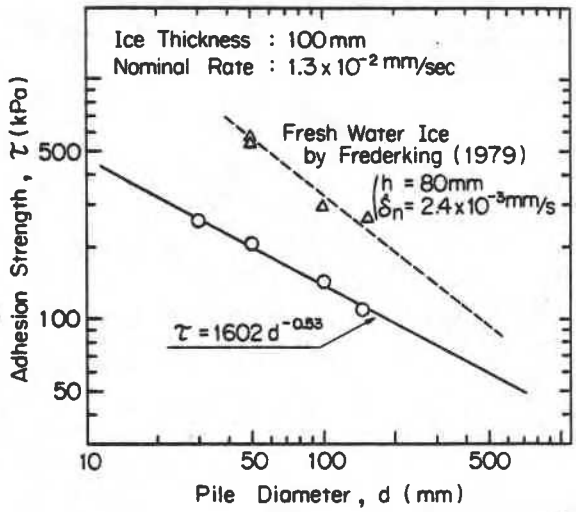

Fig.10 Adhesion strength versus pile diameter

The value of the exponent in the equation is twice that obtained for freshwater ice with the same pile diameter, but at a rate of $2.4X10^{-3}$ mm/sec which also corresponds to a maximum adhesion strength of freshwater ice (Frederking, 1979). The failure process for all freshwater ice tests was associated with the occurrence of radial cracks and formation of conical failure surface around the pile, whereas in some of the present tests with saline ice, failure was followed by the formation of circumferential cracks. Thus the difference in the values of the exponent between the two types of ice could be associated with the two different failure processes. Saeki et al. (1981) conducted pile push-out tests in naturally formed sea ice at a temperature range of -1.5 °C to -4 °C and obtained an exponent of 0.2. Differences in testing method also affect results of adhesion strength measurements considerably.

In contrast to the above described results, Frederking and Karri (1983) found no clear dependence of adhesion strength on ice thickness over the range of thickness between 50 mm and 120 mm, using freshwater ice and 100 mm diameter piles of several different materials including wood. Recently Saeki et al. (1986) have carried out extensive push-out tests using 100 mm diameter piles and observed that the adhesion strength approaches a constant when the ice thickness exceeds 60 mm.

Pile diameter effects

The adhesion strength of saline ice was plotted against the pile diameter at a nominal pile displacement rate of $1.3X10^{-2}$ mm/sec with an ice thickness of about 100 mm in Fig.10. Comparable test results for freshwater ice (Frederking, 1979) are also shown in Fig.10.

The adhesion strength is inversely proportional to approximately the square root of the pile diameter. A regression analysis gives the following best fit equation:

$$\tau = 1602\ d^{-0.53} \qquad (4)$$

where τ is in kPa and d is in mm. The exponent in the equation is different from that obtained for freshwater ice, namely -0.79, which is similar to Saeki's results (1981).

Deflection shape

Attempts were made to relate the measured deflections of the ice cover to shear and flexure in the ice. For the present test conditions, the deflection at the pile is evaluated from plate bending theory (Timoshenko and Woinowsky-Krieger, 1959),

$$W_f = \frac{P}{E}\frac{3(1-\nu^2)}{2\pi h^3}\left[\frac{a^2-b^2}{2} - 2a^2b^2(\ln\frac{b}{a})^2/(a^2-b^2)\right] \qquad (5)$$

where P is applied load, E is elastic modulus, ν is Poisson's ratio, h is ice thickness, a is radius of the tank, and b is radius of the pile. A shear deformation correction, W_s, can be calculated from

$$W_s = \frac{3}{4}\frac{P}{\pi hG}\ln(\frac{a}{r}) \qquad (6)$$

where r is distance from the pile center, G is shear modulous and $G = E/2(1+\nu)$.

The deflections of the ice cover calculated , using equation (5) and reasonable values of elastic properties of the ice, were at least one order of magnitude smaller than the measured values. Even though a reduced effective elastic modulus and the shear deformation correction, W_s, were applied, the difference from the measured values was still large. It was, therefore, decided to calculate deflection curves of the ice cover using equation (5) and equation (6) independently. This procedure was also applied successfully by Tinawi and Gagnon (1984) to compare with

Fig.11 Deflection shape

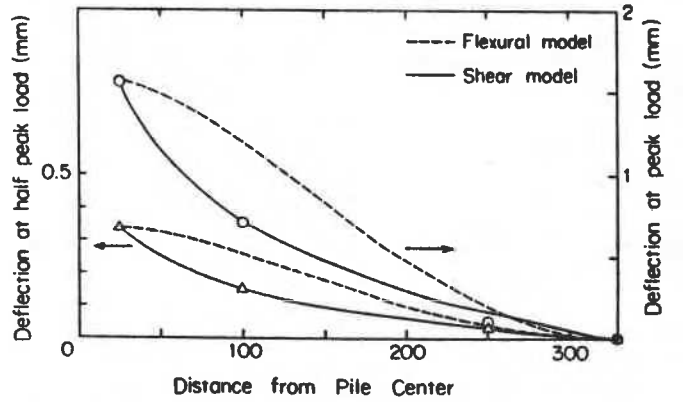

(a) test No.1

d =50mm
h =95mm
$\dot{\delta}_n$=1.3X10^{-2}mm/sec

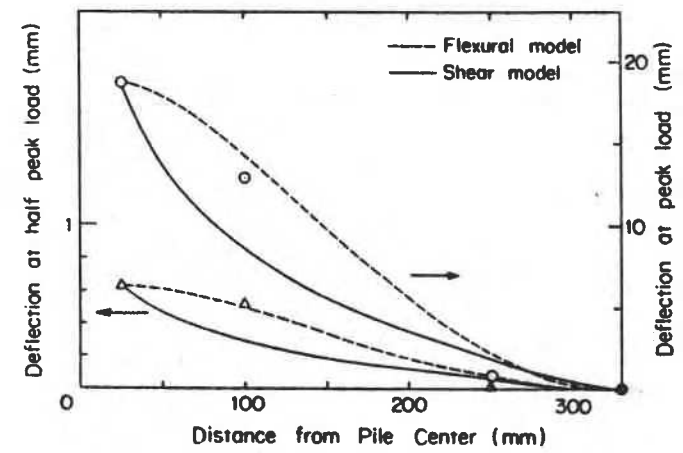

(b) test No.8

d =50mm
h =64mm
$\dot{\delta}_n$=1.3X10^{-2}mm/sec

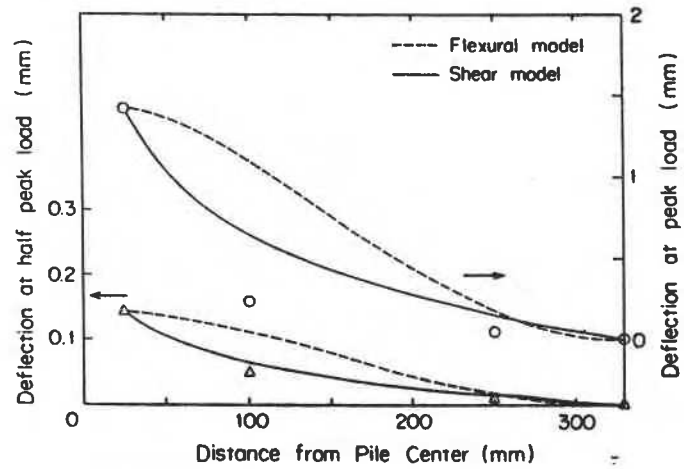

(c) test No.17

d =50mm
h =96mm
$\dot{\delta}_n$=3.5X10^{-4}mm/sec

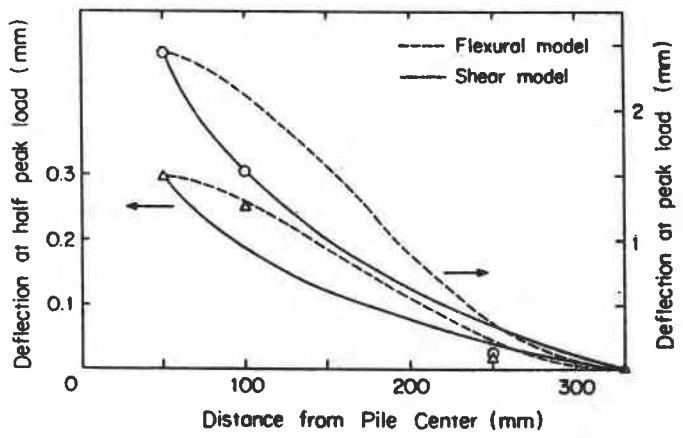

(d) test No.19

d =100mm
h = 98 mm
$\dot{\delta}_n$=1.3X10^{-2}mm/sec

the measured deflection curves on simply supported circular plates composed of similar saline ice, with a constant load applied at the center.

Fig.11 shows the deflection curves calculated in such a manner that W_f and W_s at the pile were made equal to the corresponding measured deflections both at half the peak load and at peak load. Agreement between calculated and measured values at half the peak load is remarkably good for either flexural model or shear model, but the calculated values at peak load deviate slightly from the measured values.

For test No.1 ($\dot{\delta}_n = 1.3X10^{-2}$ mm/sec), the failure was characterized by shear failure at the pile-ice interface, followed by a few radial cracks. This is clearly reflected on the measured deflection curves; i.e. the shear model accurately describes the deflections. For a thinner ice cover (Fig.11b), the failure was followed by the formation of circumferential crack. In this case good agreement between the data and the calculation was given by the flexural model.

For the slower rates (Fig.11c), no visible cracks were detected at all. The measured deflection curve agrees well with the shear model applied to the data at half the peak load, but the curve deviates significantly for the data at peak load. This difference could be due to the predominant creep deformation of the ice around the pile, as observed by Frederking (1974). This type of failure might be called shear creep failure, distinguishing it from the shear failure.

For a larger pile diameter (Fig.11d), the flexure of the ice was expected to be predominant, since more radial cracks occurred during loading. This is confirmed by the agreement between the measured values and the flexural model for the data at half the peak load. The data measured at peak load, however, fits the shear model better. This would be associated with more deterioration of the ice caused by the development of several radial cracks at failure.

Empirical formula

Based on the results presented, combining the effects of pile displacement rate, ice thickness and pile diameter on the adhesion strength, the following empirical equation can be formulated,

$$\tau = 287 \left(\frac{\dot{\delta}_n}{1.5X10^{-2}}\right)^{0.43} \left(\frac{d}{50}\right)^{-0.53} \left(\frac{h}{150}\right)^{0.80} \qquad (7)$$

for the ranges $\dot{\delta}_n < 1.5X10^{-2}$ mm/sec

$30 < d < 145$ mm

$50 < h < 170$ mm

For $\dot{\delta}_n$ greater than $1.5X10^{-2}$ mm/sec, a constant value of $1.5X10^{-2}$ mm/sec should be taken since there was no further increase in adhesion strength.

Information on measured adhesion strengths of saline ice in the field is very limited. Recently Vershinin et al. (1983) measured an adhesion strength of 194 kPa at a constant rate of 1 mm/sec for a 100 cm diameter pile frozen into natural sea ice of 115 cm thickness in the field. The mean daily temperature was -14 ℃, so that the average ice temperature could be estimated as -6 ℃, which is similar to the present test condition. Equation (7) predicts an adhesion strength of 300 kPa for those conditions. Information on pile material used in their tests is lacking, however, if the material used is assumed to be steel, the predicted value could be comparable to the measured value.

5. CONCLUSIONS

The adhesion strength of wooden piles frozen into saline ice was measured as a function of pile displacement rate, ice thickness and pile diameter. The results obtained are as follows;

(1) Two typical failure modes were observed; shear failure at the pile-ice interface and flexural failure in the ice.

(2) The adhesion strength was observed to increase with increasing pile displacement rate, increasing ice thickness and decreasing pile diameter.

(3) The adhesion strength of saline ice was found to be less by a factor of at least 3.5 than that of freshwater columnar-grained ice.

(4) At displacement rates less than 10^{-3} mm/sec the adhesion strength measured is very low, less than 100 kPa.

(5) The deflection curve analysis using flexural model and shear model was successfully applied to relate the measured deflection curve to flexure and shear in the ice.

(6) The proposed empirical equation of adhesion strength was found to give a comparable value to the field data.

ACKNOWLEDGEMENT

The authors wish to thank J. Neil, Technical Officer of DBR/NRC, for his assistance in performing the present test series.

REFERENCES

Construction Norms and Regulations, 1975. SNIP-11-57-75 Loads exerted on hydraulic structures by waves, ice and ships. National Research Council of Canada, Tech. Trans. TT-1968, 1980.

Frederking, R., 1974. Downdrag loads developed by a floating ice cover : field experiments. Can. Geotech. J., Vol.11, No.3, p.339-347.

Frederking, R., 1979. Laboratory tests on downdrag loads developed by floating ice covers on vertical piles. Proc. 5th Int. Conf. on POAC, Trondheim, Vol.II, p.1097-1110.

Frederking, R. and Karri, J., 1983. Effects of pile material and loading state on adhesive strength of piles in ice. Can. Geotech. J., Vol.20, p.673-680.

Lofquist, B., 1951. Lifting force and bearing capacity of an ice sheet. National Research Council of Canada, Tech. Trans. TT-164.

Nakawo, M. and Sinha, N. K., 1981. Growth rate and salinity profile of first-year sea ice in the high Arctic. J. Glaciol., Vol.27, No.96, p.315-330.

Oksanen, P., 1982. Adhesion strength of ice. Technical Research Center of Finland, Res. Report 123.

Sackinger, W. M. and Sackinger, P. A., 1977. Shear strength of the adfreeze bond of sea ice to structures. Proc. 4th Int. Conf. on POAC, St. John's, Vol.II, p.607-614.

Saeki, H., Ono, T. and Ozaki, A., 1981. Mechanical properties of adhesion strength to pile structures. Proc. IAHR Ice Symposium, Quebec, Vol.II, p. 641-649.

Saeki, H., Ono, T., Takeuchi, T., Kanie, S. and Nakazawa, N., 1986. Ice forces due to changes in water level and adfreeze bond strength between sea ice and various material. Proc. 5th Int. Symp. of OMAE, Tokyo, Vol.IV, p.534-540.

Sinha, N. K., 1981. Rate sensitivity of compressive strength of columnar-grained ice. Exp. Mech., Vol.21, No.6, p.209-218.

Timoshenko, S. and Woinowsky-Krieger, S., 1959. Theory of plates and shells. McGraw-Hill Book Co.

Tinawi, R. and Gagnon, L., 1984. Behaviour of sea ice plates under long term loading. Proc. IAHR Ice Symposium, Hamburg, Vol.I, p.103-112.

Vershinin, S. A. et al., 1983. Effect of an ice cover frozen to the cylindrical support of offshore oil well platforms subjected to water level fluctuation. National Research Council of Canada, Tech. Trans. TT-2041.

Weeks, W. F. and Hamilton, W. L., 1962. Petrographic characteristics of young sea ice, Point Barrow, Alaska. CRREL Res. Report 101.